Biochimica et Biophysica Acta 1837 (2014) 167–177

Contents lists available at ScienceDirect

Biochimica et Biophysica Acta

journal homepage: www.elsevier.com/locate/bbabio

# Determination of the PS I content of PS II core preparations using selective emission: A new emission of PS II at 780 nm

Jennifer Morton [a], Jeremy Hall [a], Paul Smith [a], Fusamichi Akita [b], Faisal Hammad Mekky Koua [b], Jian-Ren Shen [b], Elmars Krausz [a,*]

[a] Research School of Chemistry, Australian National University, Canberra, Australia
[b] Graduate School of Natural Science and Technology, Department of Biology, Faculty of Science, Okayama University, Okayama, Japan

ARTICLE INFO

*Article history:*
Received 12 July 2013
Received in revised form 6 September 2013
Accepted 11 September 2013
Available online 20 September 2013

*Keywords:*
Photosystem I
Photosystem II
Fluorescence
Fluorescence line-narrowing
Spectral hole-burning

ABSTRACT

Routinely prepared PS II core samples are often contaminated by a significant (~1–5%) fraction of PS I, as well as related proteins. This contamination is of little importance in many experiments, but masks the optical behaviour of the deep red state in PS II, which absorbs in the same spectral range (700–730 nm) as PS I (Hughes et al. 2006). When contamination levels are less than ~1%, it becomes difficult to quantify the PS I related components by gel-based, chromatographic, circular dichroism or EPR techniques. We have developed a fluorescence-based technique, taking advantage of the *distinctively different* low-temperature emission characteristics of PS II and PS I when excited near 700 nm. The approach has the advantage of providing the relative concentration of the two photosystems in a single spectral measurement. A sensitivity limit of 0.01% PS I (or better) can be achieved. The procedure is applied to PS II core preparations from spinach and *Thermosynechococcus vulcanus*. Measurements made of *T. vulcanus* PS II preparations prepared by re-dissolving crystallised material indicate a low but measurable PS I related content. The analysis provides strong evidence for a previously unreported fluorescence of PS II cores peaking near 780 nm. The excitation dependence of this emission as well as its appearance in both low PS I cyanobacterial and plant based PS II core preparations suggests its association with the deep red state of PS II.



## 1. Introduction

PS II core complexes are widely utilised to study fundamental processes in PS II as it is the minimal photosynthetic assembly that can evolve oxygen. PS II cores have the CP43 and CP47 proximal antennae intimately attached to its D1/D2/cyt$_{b559}$ reaction centre protein assembly. It is possible to isolate D1/D2/cyt$_{b559}$ reaction centre assemblies [1]. They undergo charge separation, but do not bind plastoquinones and their tyrosines are not photoactive. Additionally, they do not retain the oxygen-evolving centre containing the catalytic $Mn_4CaO_5$ cluster. We have shown [2] that the reaction centre present in PS II core complexes differs with that of isolated D1/D2/cyt$_{b559}$ in their absorption characteristics, particularly in the 700–730 nm range.

PS II core complexes can be prepared to have an oxygen-evolving capacity approaching that of membrane bound PS II or thylakoids. Core complexes isolated from *Thermosynechococcus vulcanus* and closely related thermophiles, have been successfully crystallised, allowing a crystal structure determination [3] to atomic resolution (1.9 Å). These crystal structures have in turn provided great impetus to theoretical and experimental studies; the primary goals being the determination of the mechanism of catalytic water oxidation at the oxygen evolving centre as well as a detailed electronic understanding of light harvesting and reaction centre processes.

Core complexes derived from plants are usually prepared via a two-step process. Membrane bound PS II is first prepared and isolated (these often are called BBYs). These preparations contain light harvesting complexes (LHCs) and may incorporate a significant amount of PS I. A second detergent solubilisation step and a chromatographic separation then provide purified PS II core complexes.

Separation of cyanobacterial PS II core complexes does not involve the initial membrane-bound PS II preparation stage. Chromatographic separation of cyanobacterial PS II cores can be assisted by the creation of an appropriate histidine-tagging mutant, which can then be separated via binding to a nickel-affinity column. PS II cores prepared from plant sources may be contaminated by both LHCs and PS I. Cyanobacteria do not typically have LHCs (*Acaryochloris marina* being an notable exception [4]) but may be contaminated by PS I and phycobillins. The PS I content in cyanobacterial thylakoids is typically higher than that in plants, relative to PS II.

The PS I content of a PS II core preparation can be estimated by gel-based methods and EPR. We have also utilised the distinctive circular dichroism (CD) signature of the 'red trap' states of PS I to provide upper bounds for PS I related contamination [5]. EPR is sensitive to the presence of $P700^+$, which is generated by mild oxidation of a PS I sample with ferricyanide. However, we have found that when the concentration of PS I is below ~2%, the above methods become impractical. In plant

* Corresponding author. Fax: +61 2 6125 0750.
*E-mail address:* krausz@rsc.anu.edu.au (E. Krausz).

0005-2728/$ – see front matter © 2013 Elsevier B.V. All rights reserved.
http://dx.doi.org/10.1016/j.bbabio.2013.09.008

systems, a preparation may have some PS I but also contain LHCs detached from the PS I core. These also absorb in the 700–730 nm region, giving rise to PS I-like long wavelength emission.

PS I does not fluoresce well at room temperature but fluoresces quite strongly at low temperatures, having a characteristically broad emission peak between 730 and 740 nm. The emission characteristics vary somewhat with organism [6]. PS I samples in which P700 is oxidised show a weakened emission, slightly shifted to the blue [7]. PS II fluorescence at 77 K exhibits the well-known peaks at 685 nm and 695 nm, labelled in the literature as F685 and F685. PS II fluorescence is strongly temperature dependent [8,9] and the F685/F695 ratio varies significantly with both the organism and the state of preparation of the sample. Fig. 1 provides non-resonantly excited, 8 K and 77 K emission spectra of a typical membrane (BBY) preparation, a PS I preparation and a PS II core preparation isolated from spinach, normalised to the same number of detected quanta.

The emission of our spinach PS I preparation clearly shows a strong peak near 680 nm, which is a characteristic of LHCII, as well as a broad PS I emission peak near 735 nm. Although the latter emission overlaps with vibrational sideline bands arising from F685 and F695 bands of PS II, it is possible [10] to estimate the PS I content of a PS II preparation by fitting the full emission spectra with profiles associated with PS I and PS II. The BBY sample emission spectrum (Fig. 1) indicates a significant PS I content and such a 'fitting' approach is of value for high PS I content samples. However, the presence of emission intensity arising from light-harvesting assemblies LHCII, CP29 etc. which have vibrational sideband features in the 730–740 nm region would make such an approach difficult and somewhat ambiguous. Although Fig. 1 shows there is significant LHCII content of our PS I preparation, the temperature dependence of the emission between 5 K and 77 K (Fig. 1 and Supplementary data Fig. S1) shows that many of these LHCIIs are attached to PS I. A significant fraction of our sample is likely to be of the PS I-$(LHCII)_3$ type recently discussed [11]. Although there are now better ways to prepare plant PS I preparations [12], the technique chosen has the advantage of proceeding through a Triton detergent solubilisation step, which is also utilised in the preparation of PS II plant core complexes (in the BBY preparation step).

Quantification of low-PS I content using a simple (non-resonant excitation) fluorescence excitation technique is not reliable. The PS I emission profile varies with the form(s) of PS I present in both plants and cyanobacteria [6,13,12]. Additionally, the overall emission from PS II is both strongly temperature dependent and the emission profile of PS II itself varies with the degree of solubilisation of the proteins. The actual PS I related species present in plant PS II core preparations are potentially more solubilised than those in a purpose-made PS I preparation. These more solubilised PS I related species may emit with their own peak positions and linewidths. As mentioned above, the PS I emission profile varies when P700 is oxidised. In a PS II preparation containing PS I exposed to light, the P700 present may become partially oxidised.

It has become important for us to quantify (and subsequently attempt to reduce) the PS I content of PS II preparations, in order to make systematic quantitative measurements on the deep red state (DRS) in PS II cores [14]. This broad state in PS II spinach cores extends to ~730 nm and has an estimated absorption intensity of ~0.15 $Q_y$ chl-a. The PS II core samples used in the original work were estimated to have <1% PS I. This was determined by (the absence of) measureable CD signatures in the 690–730 nm region. This procedure required careful low-temperature measurements on thick and very concentrated PS II core samples. The low level of contamination in the particular core complex sample utilised did indeed preclude the possibility of significant absorption in the 700–730 nm region to be associated with PS I or its related LHC fragments.

The initial observation of the DRS in PS II, along with its associated photochemical activity, pointed to the DRS being the lowest excited state of PS II. It was also suggested that this state may give rise to emission that extended beyond 730 nm. In the process of looking for this putative DRS emission, low temperature excitation of a PS II core sample from spinach via Ti:S laser excitation beyond 700 nm was undertaken [15]. These experiments gave rise to an easily measureable emission, but its spectral features were attributable to a PS I related contaminant.

In this paper we develop a fluorescence protocol that enables the determination of the PS I/PS II ratio of a sample when the PS I content is well below 5%. This determination is made for a range of PS II core complex preparations, and has allowed us to identify preparations with particularly low PS I related content. Furthermore, in emission spectra of PS II cores with very low PS I, we have been able to identify an emission arising from excitation of PS II core samples with 700–720 nm radiation. The systematics of the emission properties help enable us to determine that it is not associated with PS I and indeed arises from PS II.

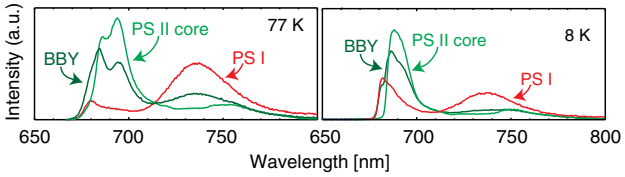


**Fig. 1.** Emission spectra of membrane particles (BBYs) PS II cores and PS I prepared from spinach at 77 K (left) and 8 K (right). Spectra are corrected for response of the system and normalised to the same number of emitted quanta.

## 2. Materials and methods

Emission spectra were measured on a laboratory-constructed spectrometer based on a high-resolution Spex 1404, 0.85 M double monochromator incorporating an additional internal spatial filter middle stage. This monochromator provides an extremely high stray light rejection ratio of $1{:}10^{18}$. Gratings blazed at 750 nm with 1200 lines/mm were utilised along with a red sensitive RCA C31034 or Hamamatsu R943-02 photomultiplier. This system provided good sensitivity to beyond 800 nm, whilst having more than adequate resolution (0.4 nm/mm slit width). The wavelength sensitivity of the system was calibrated with a black body source and spectra are corrected for system response. The photosystem samples were loaded into a 200–400 μ thick quartz 'split cell' of our own design [16,17]. The cryoprotectant utilised was a 1:1 mixture of ethylene glycol:glycerol, made up to have a final 40% v:v fraction, providing samples of high optical quality.

Cryogenic temperatures were routinely enabled by a simple and efficient quartz flow tube system [18] operating with either liquid nitrogen or liquid helium. The excitation source was either a 1 mW helium-neon laser at 632.8 nm or a Ti:S laser (Schwartz EO) pumped with a Continuum Verdi G CW laser operating at 532 nm. The laser was defocussed to provide a uniform 3 mm ϕ excitation beam. Additional absorption and emission measurements were made on an alternate apparatus previously described [14]. This utilised a Spex 0.25 mm double monochromator fitted with a 250 W tungsten-halogen lamp, providing an extremely stable, spectrally pure and versatile broadband excitation source along with a 0.75 M Spex single monochromator to analyse the emission.

PS II membrane and core complexes isolated from spinach were prepared by the method previously described [19]. A PS I sample was isolated from spinach using the procedure previously described [20,21]. *T. vulcanus* core complex samples were prepared as described [22,23]. In order to provide samples with less PS I content, crystals of PS II were re-dissolved in a buffer containing 30 mM Mes (pH 6.0), 20 mM NaCl, and 3 mM $CaCl_2$.

## 3. Results

### 3.1. Absorption and selective emission of PS II and PS I

We have shown, from low temperature absorption, spectral hole-burning (SHB) and fluorescence line narrowing (FLN) [24,25,14] experiments, that absorption, and subsequent emission, of the CP47 'trap'

state in PS II spinach cores falls gradually from 690 nm, and extends to a limit of ~704 nm. Beyond this point, absorption of the deep red state (DRS) extends to 730 nm.

Absorption of plant and cyanobacterial PS I typically extends to 725 nm and beyond [6,12,13]. The details depend on the particular organism and the organisation (monomer/trimer/LHC etc.) of the PS I assembly. Absorption of PS I is relatively uniform (compared to PS II) in the 690–720 nm region. Fig. 2 shows the absorption and emission spectra of spinach and *T. vulcanus* PS 1 and PS II at 77 K. Absorption spectra are placed on a molar extinction scale allowing the relative absorption of PS I to PS II to be compared.

In exciting PS II core preparations containing PS I with radiation in the 695–720 nm region, it is possible to enhance, very significantly, the intensity of the fluorescence component due to PS I compared to PS II, by selection of the excitation wavelength to a region where PS I absorption dominates. For example, at 698 nm, the relative absorption of PS I to PS I can be estimated to be ~50:1 (Fig. 2).

### 3.1.1. Excitation wavelength dependence of PS II emission

In addition to the different wavelength sensitivities in absorption strength (and subsequent emission intensity) between the two photosystems, the emission spectra of PS I and PS II differ in a key fundamental characteristic. Emission from the CP47 trap state in PS II is substantially *inhomogeneously* broadened, whereas PS I emission is dominantly *homogeneously* broadened [26]. These characteristics are illustrated in Fig. 3. These characteristics are evident in the Stokes shifts between absorption and emission and are explored in more detail by laser selective spectroscopies [27,28,17] such as FLN and SHB, which probe homogeneous and inhomogeneous broadening directly. The Small/Jankowiak [26,29] groups in particular have investigated the 'red trap' states in PS I from *T. elongatus* and *Syn. 6803* in detail. Yang et al. [30] have attempted to identify the 'red trap' pigments, although a consensus on the number and location of trap states does not seem to have been achieved.

However, the significance to this work is that fluorescence spectra, when directly excited from the *lowest (emitting) excited state* of a system become markedly different for the two situations, i.e. homogeneous vs inhomogeneous broadening. In the inhomogeneous broadening case, the electronic origin region of each site (Schematic in Fig. 4) carries significant intensity and emission becomes dominantly resonant with the excitation light. Resonant emission cannot normally be seen, as it is overwhelmed with excitation light at (or very near to) the same wavelength. However, strongly *narrowed* vibrational sideband features (as FLN) can be seen. These features are shifted from the exciting light energy by a vibrational quantum $\nu_{ground}$ of the chromophore, as illustrated in Fig. 4. There are many vibrational modes that couple to a chlorophyll $Q_y$ excitation. Fig. 5 reproduces previously published, highly resolved FLN spectra of *isolated* CP47 preparations, demonstrating the pattern of sharp vibrational sidelines characteristic of chl-a. Each sharp electronic origin (Zero Phonon Line or ZPL) and its vibrational sideline is also accompanied by a phonon wing (see Fig. 6). The intensity of the phonon wing is governed by the electron–phonon coupling in the system, analogously to the Frank–Condon factors for (molecular) vibrational sidelines in electronic absorption spectra. The sharp vibrational sidelines correspond to emission from a subset of the (CP47) assemblies that have their ZPL at the energy determined by the exciting laser.

The linewidth of the vibrational sideline is governed, at low temperatures, by vibrational relaxation times, which are typically ~1–3 ps in chlorophyll-like systems, an example being vibrational sideholes in water soluble chlorophyll transport protein [31]. Thus the linewidth of the FLN vibrational sideline, when excited by a narrow band laser, will be of the order of a few $cm^{-1}$ and has a Lorentzian (i.e. lifetime limited) lineshape. At higher temperatures, the line remains Lorentzian but its width increases rapidly due to vibrational relaxation and dephasing processes.

An added complexity in interpreting an FLN spectrum is that the line narrowing described above occurs *in competition* with spectral hole-burning (SHB). SHB depletes the absorption of (CP47) pigment species in the PS II core complex having a ZPL at the laser wavelength used in excitation. Special techniques can be used to recover the FLN spectra corrected for the effects of hole-burning in antenna systems [32] but CCD based fluorescence spectrometers are needed so that the amount of exciting light required to accumulate an FLN spectrum is minimised. We have shown [33] SHB in PS II core complexes to be particularly efficient, with the quantum efficiency (QE) in some circumstances approaching unity [24]. Obtaining sharp-line FLN is thus more difficult, if not impossible, as all the sites of the inhomogeneous distribution having their ZPLs at the excitation wavelength will become depleted via SHB *before* sharp-line FLN spectra can be accumulated.

When a broader spectral width excitation source is utilised, low-resolution FLN spectra of PS II cores can indeed be obtained [34]. SHB is significantly reduced by using a broadband excitation source as a far wider range of single sites are accessed. For example, the linewidth of the ZPL for a strongly-emitting chlorophyll at low temperatures can be extremely small, at ~0.001 $cm^{-1}$ FWHM or less. If an excitation source of 10 $cm^{-1}$ width is used, the same incident power is distributed to ~$10^4$ more sites, compared to those accessed by a narrow-band (i.e. <0.001 $cm^{-1}$ FWHM) laser. The resolution of the FLN spectra obtained with broadband excitation becomes determined by the spectral width of the excitation source.

The (intentionally) low-resolution FLN spectra of PS II cores previously published [34] are reproduced in Fig. 5. They correspond well to the published FLN spectra of *isolated CP47* [35] when the latter spectra are convoluted with a Voigt function so as to account for linewidth of excitation used (~50 $cm^{-1}$ FWHM). The low-resolution experiment on PS II cores utilised a far lower excitation power (6 μW/$cm^2$) compared to the 100 μW/$cm^2$ value used in the high-resolution FLN experiment on isolated CP47. The two main features seen in low-resolution FLN spectra of PS II cores occur at ~760 $cm^{-1}$ and ~1200 $cm^{-1}$ shifts from the excitation frequency. We refer to these as the V1 and V2 sideband features in this manuscript; other weaker sideband features, corresponding to other vibrational quanta in the ground state (Fig. 4) behave analogously.

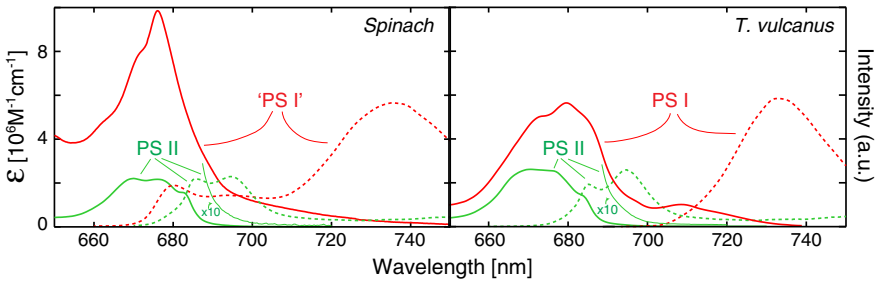


**Fig. 2.** Scaled absorption, solid lines & l.h. scale with corrected emission, dashed lines & r.h. scale of PS I (red) and PS II cores (green) of spinach (left panel) and *T. vulcanus* (right panel) at 77 K. *T. vulcanus* molar extinction values are room temperature values reported for *Thermosynechococcus elongatus* [46]. Spinach PS II extinction coefficients are taken from reported values [2] and corresponding values for spinach PS I are estimated from the integrated area of the $Q_y$ band and scaling it to the measured chlorophyll content of the preparation (see text).

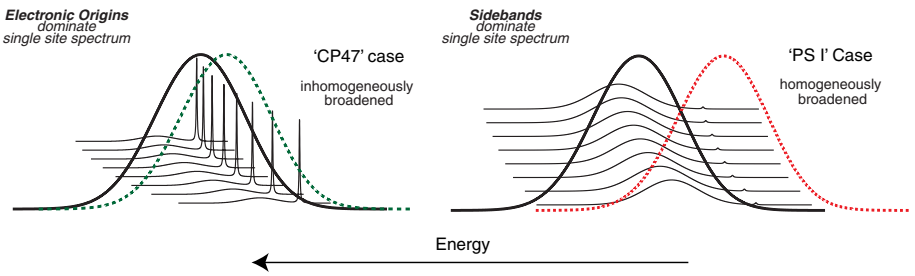


**Fig. 3.** Schematic of low temperature absorption (solid line) and emission (dashed line), for the inhomogeneous ('CP47') and homogeneous ('PS I') broadening cases. Individual pigments have different excitation energies, giving rise to inhomogeneous broadening. Homogeneous broadening in PS I is due to strong electron–phonon coupling (see text).

With *laser* excitation of PS II cores at 698 nm at 5 K, narrow FLN side-features are entirely absent in our spectra, although the spectrometer itself is fully capable of resolving features narrower than 1 $cm^{-1}$. Additionally, Fig. 5 shows that the lineshape and intensity of the V1 and V2 sideband features are strongly temperature dependent in the 5–40 K range. At the lowest temperatures, V1 and V2 are *weaker and red shifted* compared to the bands as seen at higher temperatures. When broadband excitation at 698 nm is used to excite FLN, there is virtually no temperature dependence of the V1 and V2 features over the 1.7–35 K range (Supplementary Fig. S2). V1 and V2 do broaden significantly above 40 K. Parallel behaviour is seen in corresponding temperature dependent broadband 698 nm excited emission spectra of *T. vulcanus* PS II cores (Supplementary Fig. S2).

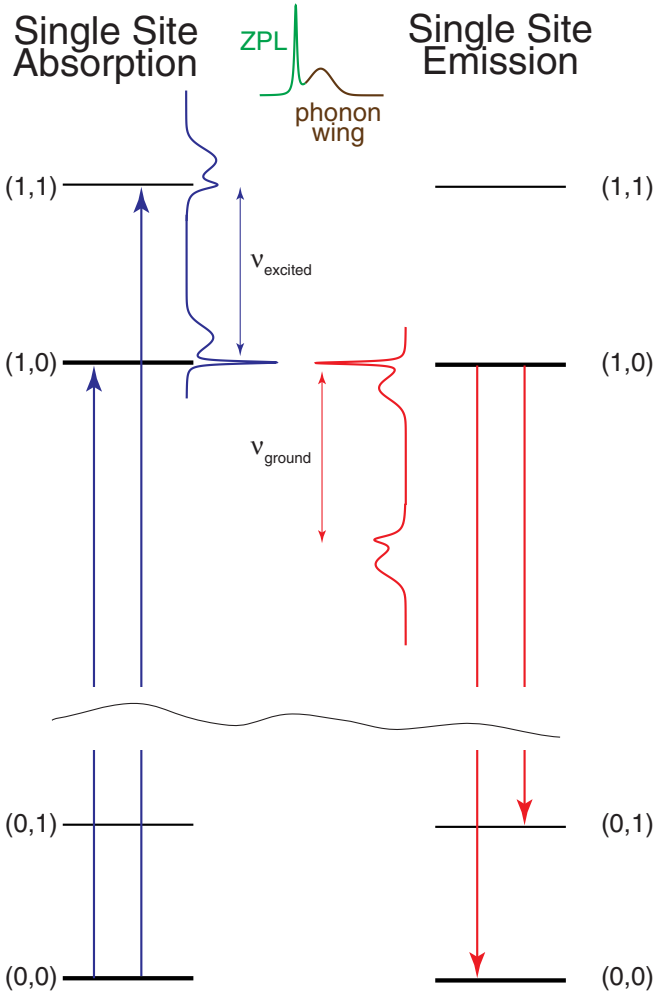


**Fig. 4.** A schematic of low-temperature chlorophyll-like single site absorption and emission of electronic origins and their vibrational sidelines (see text). Each site has a narrow electronic ZPL, accompanied by a phonon wing, being crudely represented by a Gaussian. Phonon wings typically peak in the 20–100 $cm^{-1}$ range and their intensity is dependent on the electron–phonon coupling. Vibrational sidelines $\nu$ are shifted 400–1500 $cm^{-1}$ from the origin and also exhibit phonon-wings. Vibrational sidelines are typically ~1-10 $cm^{-1}$ at very low temperatures due to vibrational relaxation in the ~ps timescale.

The phenomena seen above can be attributed to efficient SHB processes, previously identified in PS II cores. Upon warming to the 20–40 K range, the reverse of SHB, spectral hole-filling [36,24], out-competes SHB, leading to the absorption strength at the excitation laser wavelength being recovered. We have shown [37] that PS II core complexes exhibit more rapid hole-filling as well as a strong ($\propto T^2$) dependence of the hole width with temperature than seen in studies of typical light harvesting complexes [27]. This enhanced hole-filling process in PS II cores is responsible for the changes in laser excited emission spectra seen in Fig. 5. Broadband excited spectra (Supplementary Fig. S2) show that there is no *intrinsic* change in emission intensity in the low temperature range.

A *decrease* in the intensity of FLN features with lowering temperature seems counter-intuitive, but an interplay between FLN and SHB processes as suggested above has been reported [38] for the related Zn-cytochrome-c system. Supplementary Fig. S12 demonstrates the dramatic increase in sensitivity towards the PS I content in a PS II core sample upon increasing the power density of laser excitation in an experiment performed at 7 K. This relative increase in PS I emission, relative to PS II, can be attributed to SHB processes in PS II significantly reducing the absorption of PS II at the laser wavelength, with absorption due to PS I not being strongly affected.

As well as the fluorescence excited by absorption into those sites whose ZPL is *resonant* with the laser energy (scenario A in Fig. 6), another (far broader) range of sites, i.e. those which have significant phonon wing absorption at the laser wavelength, will also be excited. Subsequent emission from these sites, at temperatures lower than phonon excitation energies, arises from the ZPLs of this distribution of sites. This process gives rise to a second, lower energy wing in FLN spectra as depicted in scenario B of Fig. 6. The lower energy wing of the 'double wing' originates from sites whose *phonon wing* is excited by the laser. This lower component of the 'double wing' is broader than the primary phonon wing, as it is a convolution of the width of the originally excited (phonon wing) and the profile of the emission (ZPL + phonon wing) arising from these sites. Fig. 6 scenario B depicts how the lower wing is shifted from the primary wing by an amount comparable to the phonon wing peak frequency.

In the presence of strong SHB, the entire population of sites whose ZPL is resonant with the laser frequency becomes depleted. Consequently there is no (ZPL + phonon wing) emission from these sites. Residual emission will come from the *phonon wing excited* emission, as depicted in scenario C of Fig. 6. If broadband excitation is utilised and SHB thus minimised, then emission will simply be a broadened version of the FLN in scenario B.

To summarise, there is not temperature at which we actually see narrow vibrational sideline FLN features appear in our laser-excited spectra (see Fig. 5). At ~30 K, the broadband and laser-excited spectra

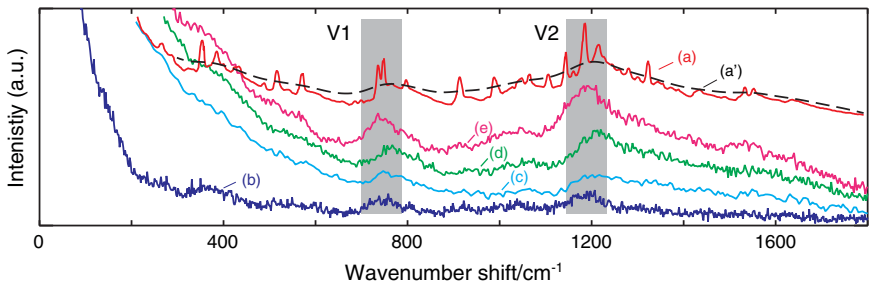


**Fig. 5.** Trace a) is the FLN spectrum at 8 K of an isolated CP47 preparation reported [35]. The dashed line (a′) is the same spectrum convoluted with a Voigt profile of FWHM width 50 $cm^{-1}$ (see text). The strongest features occur in the regions marked V1 and V2. Trace (b) is the low-resolution FLN spectrum of PS II cores at 1.7 K reported [8]. Traces (c), (d) and (e) are 698 nm laser-excited FLN spectra of PS II core sample (b) at 11 K, 30 K and 38 K. Incident fluence was 180–200 $mW/cm^2$ (see text).

are practically identical (see Supplementary Fig. S3). This indicates that, at temperatures where hole-filling becomes dominant over SHB leading to more absorption and therefore more emission, there is a rapid shortening of the dephasing time, which strongly broadens any re-appearing ZPLs [36]. Thus, rather than *narrow* vibrational sideband features being seen, ZPL intensity is re-gained in a strongly broadened form. This recovered ZPL intensity, along with the phonon-wing intensity coming with it, leads to the overall increase in intensity and blue shift of the V1/V2 regions with increasing temperature, seen in Fig. 5.

The *T. vulcanus* PS II core data in Fig. 7 exhibit the temperature dependent phenomenology described by above scenarios. This sample additionally exhibits a broad emission band near 740 nm, indicative of PS I content. The phenomena shown in Fig. 7 are reproduced at other

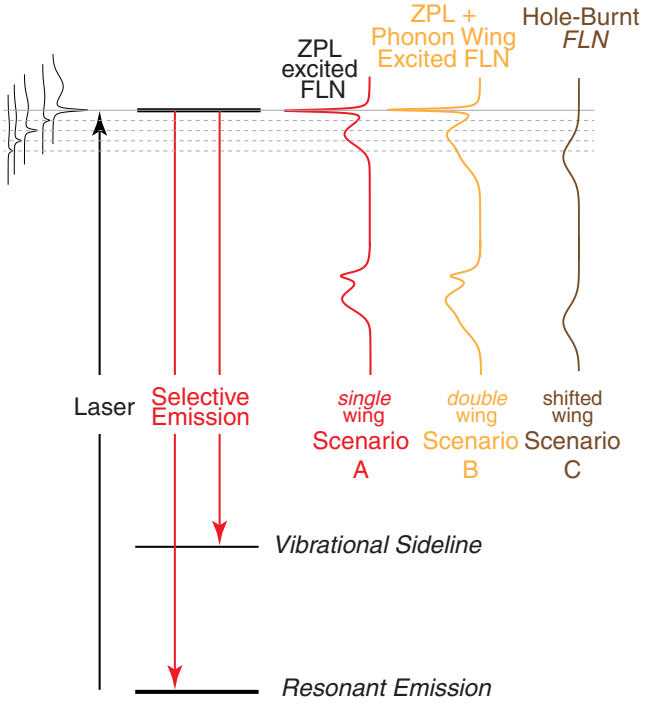


**Fig. 6.** FLN features become modified in the presence of strong spectral hole-burning (SHB). Scenario A is the simplest case, in the absence of SHB, and when only the ZPL of a subset of pigment sites is excited. FLN spectra would then exhibit relatively sharp vibrational sidelines, these having phonon wings mirroring those of the ZPL. Scenario B accounts for phonon wings of the ZPLs of other subsets of pigments also being excited. Relaxation occurs before emission from these sites, giving rise to a second, lower energy FLN wing (see text). When strong SHB occurs (scenario C) the sites having ZPLs resonant with the laser wavelength are strongly depleted. No sharp vibrational sidelines are then seen. Only the second part of the double wing in scenario B survives, giving rise to a relatively broad peak at lower average energy compared to FLN features in scenario B. This selective emission arises from those sites whose phonon wing (but not ZPL) has significant absorption strength at the laser energy.

excitation wavelengths and with other PS II samples, in an entirely systematic way.

### 3.1.2. Excitation wavelength dependence of PS I emission

The excitation wavelength dependence and temperature dependence of PS I emission are more straightforward. As this system is strongly homogeneously broadened, with weak electronic origins, SHB and FLN processes are less important and the system does not exhibit the complex phenomenology of PS II described above. We have previously reported [15] the excitation dependence of low temperature emission using 707–725 nm laser excitation of a spinach PS II core complex sample which was concluded to have a PS I related contaminant (i.e. LHC-730). Fig. 8 shows a detailed excitation wavelength dependence of the PS 1 isolated from spinach, which shows an analogous broad, Stokes shifted emission. Corresponding spectra of PS 1 in *T. vulcanus* are entirely analogous and are provided in the Supplementary data (Fig. S4).

PS I emission is homogeneously broadened, exhibiting a substantial Stokes shift. Emission intensity resonant near the excitation wavelength is low, even when exciting directly into the emitting excited state. Such resonant excitation (excitation into the emitting state) then leads, in contrast to PS II, to a characteristically broad emission. This emission becomes only slightly narrower upon excitation at longer wavelengths, with the peak gradually tracking to lower energy when longer wavelength excitation is used. This reflects the inhomogeneous component of the dominantly homogeneous broadening in PS I.

Note that the V1/V2 sidebands obtained by resonant excitation of PS II maintain a *constant* energy displacement (i.e. that of a vibrational quantum) from the exciting wavelength. In this characteristic, they behave like Raman peaks. However, fluorescence and Raman processes have distinctly different selection rules and dynamics. Only a single vibration or phonon is excited in the Raman process, with combination and overtone bands being characteristically weak. Chlorophyll FLN typically exhibits vibrational sidelines combined with a phonon of comparable intensity. Such a process is forbidden in the Raman process. In Raman spectra, phonon scattering is seen close to the laser line with sharp vibrational sidelines appearing at greater energy displacements from the laser line. In Raman spectra, these characteristic sharp vibrational sideline peaks do not have an associated phonon wing, as seen in FLN. Additionally, Raman scattering does not show dramatic broadening in the 2 K–70 K temperature range, nor does it have the very strong wavelength dependence of scattering intensity observed in our spectra. Thus we can exclude the possibility of Raman processes contributing significantly to the emission phenomena reported.

As mentioned in 3.1.1, weak SHB and FLN phenomenologies only become evident in PS I when exciting at the very low energy edge of PS I absorption [26,29]. The overall behaviour of PS I emission is consistent with the 'homogeneously broadened' schematic in Fig. 3.

### 3.1.3. Excitation wavelength dependence of PS II emission

A detailed analysis of the complex phenomenology exhibited by PS II emission is ultimately well beyond the scope of this paper. The reader is

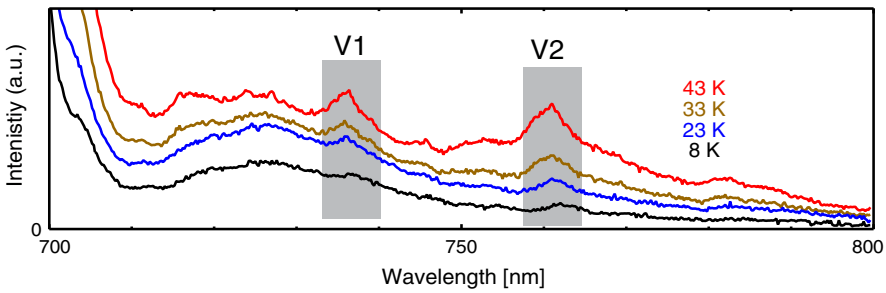


**Fig. 7.** Temperature dependence of selective emission of a *T. vulcanus* sample excited by ~200 mW/cm$^2$ laser excitation at 698 nm. The behaviour of V1 and V2 parallels that in spinach (see Fig. 5) and there is an additional broad emission feature near 730 nm due to PS I.

referred to reviews and texts [39,40,27,28,17] for a more comprehensive discussion of FLN and SHB techniques. Our focus is to effectively detect and quantify the PS I content and purity of PS II samples.

We have established (Figs. 5 & 7) that low-temperature excitation of PS II samples in the 700 nm region gives rise to characteristic broadband emission from PS I related contaminants, as well as the FLN sideband features (i.e. V1/V2 etc.) arising from CP47 in PS II cores. These latter emission features are undeniably associated with PS II and are, apart from competing SHB processes, independent of temperature in the 1.7–35 K range (Supplementary Fig. S2). Thus, these features can be used to estimate the PS II concentration, especially as total sample absorption in the 700 nm region is inherently low, obviating any fluorescence re-absorption.

Fig. 9 shows selective emission spectra of PS II core samples having a measurable PS I content. These spectra utilise weak, broadband excitation where SHB processes are minimised. This PS I content becomes more clearly evident with excitation > 705 nm, where a broad PS I band persists after the disappearance of the CP47 V1/V2 FLN sideband structure of PS II.

The sensitivity of selective emission spectra towards PS I becomes dramatically increased (Fig. 10) by using high power-density laser excitation. In these circumstances strong SHB reduces PS II core absorption at the laser wavelength. PS I does not suffer SHB to a significant extent and PS I fluorescence becomes (relatively) more than an order of magnitude more visible. In the *T. vulcanus* spectra broadband excited at 698 nm, PS I emission is barely visible whereas in laser excited spectra the 735 nm peak is absolutely dominant.

Fig. 12 shows the wavelength-dependent selective emission spectra of PS II core complex samples at 8 K of spinach and *T. vulcanus* having low PS I content. The laser excitation utilised ensures an enhanced visibility of any PS I content via SHB processes, as seen in Fig. 10. CP47 V1/V2 FLN structures move, as expected, to longer wavelengths and precisely follow the excitation wavelength. In both systems, there is a broad (~500 cm$^{-1}$ FWHM) residual emission near 780 nm, which becomes more visible via excitation in the 710–720 nm region. The emission vanishes with excitation beyond 720 nm in both plant and cyanobacterial samples. Supplementary Fig. S5 shows the deep red emission region in *T. vulcanus* in more detail. At each excitation wavelength, the band is least-squared fitted to a Gaussian. The position, width and amplitude are provided in Supplementary Table S1. The band position is reproducibly fitted to 780 ± 2 nm with a FWHM width of 22 ± 3 nm. The spectra in spinach are similar but any fitting is hampered by the persistence of CP47 V1/V2 FLN features. This previously unreported emission will be discussed further in Section 4.

### *3.1.4. Absorption and selective emission of other potential fluorescent contaminants*

A remaining concern is with regard to any other species that may contribute to selective emission, when excited in the 698–730 nm region. In plant systems, LHC II, CP29 and other LHCs exhibiting absorption and emission near 680 nm are not excited by excitation in the 698–720 nm region. This was confirmed by comparing selective emission spectra of BBYs and PS II cores excited at 698 nm. The BBYs contain a significant fraction of LHC II but the PS II core sample far less. No difference was seen in the V1/V2 selective emission features. Thus identification and quantification of PS II via the V1/V2 features is not compromised by the presence of these LHCs. A similar exclusion applies to any phycobillins present in cyanobacterial *T. vulcanus*.

Species absorbing significantly in the 698–700 nm region are PS I, in its various solubilised/oxidised forms (trimer/monomer) and in plant systems, LHCIs associated with PS I that may have become detached from a native PS I assembly. These latter species also exhibit homogeneously broadened 'red trap' states [6] and give rise to broad, Stokes shifted emission. The low temperature QE of emission of these 'red trap' states is likely to be similar. To a first order approximation, the molar extinction of each 'red trap' will be that of that associated with ~2 (relatively broad) chl-as. An estimate of ε ~100,000 M$^{-1}$ cm$^{-1}$ for each 'red trap' pair is appropriate.

Thus, for this case regardless of the *particular* form of the 'PS I related' contaminant present, they can be considered to absorb, through the 'red trap', to a similar extent and have a broad, Stokes shifted, 'red trap'

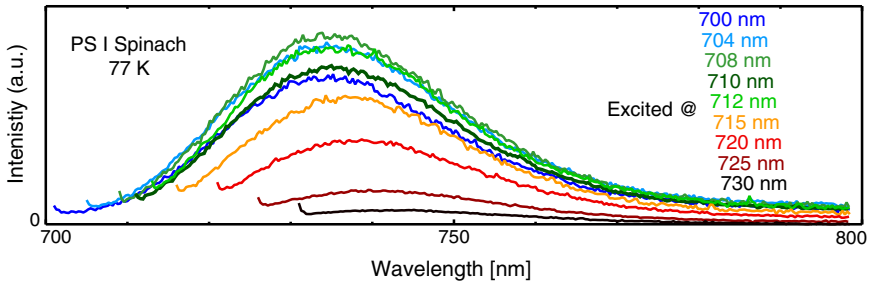


**Fig. 8.** Wavelength dependence of selective emission at 77 K of a spinach PS I sample (see text) excited by 70–150 mW/cm$^2$ laser excitation at the wavelengths indicated. Spectra are corrected for the power of the laser.

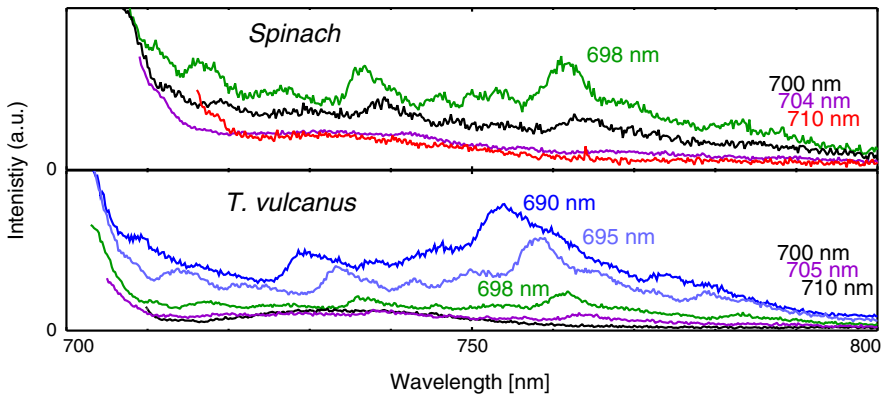


**Fig. 9.** Selective emission at 1.7 K of a spinach sample (a) (upper) and non-recrystallised *T. vulcanus* (lower) PS II samples (see text) excited by 6 μW/cm$^2$ broadband excitation at the wavelengths indicated.

emission with a similar intensity. To our purposes, the precise nature of the PS I related contaminant in plants is then not critical.

We particularly look to identify absorption features seen in the 700–730 nm region which are due to the DRS of PS II and that do not arise from PS I, by calibrating the resonantly excited emission of the PS II sample, with and without known amounts of purposely added PS I. Regardless of the precise form of the PS I related contaminant, its long-wavelength absorbing component is effectively monitored, and to an equivalent extent, by monitoring the amplitude of the characteristic Stokes-shifted emission. Additionally, this broadband PS I emission can be calibrated against the (purely PS II) V1/V2 sideband features which are proportional to the PS II content.

The low temperature absorption of spinach PS II at 698 nm has an ε ~20,000 M$^{-1}$ cm$^{-1}$, falling to ~10,000 M$^{-1}$ cm$^{-1}$ at 705 nm, the later value [14] being attributable entirely to the DRS of PS II. Taking each PS I 'red trap' to have an (relatively uniform) ε ~100,000 M$^{-1}$ cm$^{-1}$ in the 698–705 region, allows us to vary the PS I/PS II *absorption ratio* from an ~10 at 698 nm to much higher values near 704 nm (i.e. the established limit of the CP47 absorption). Note that at 698 nm half of the absorption is due to CP47 and the remainder due to the DRS.

Emission efficiencies of PS II and PS I at low temperatures [41] are comparable (~10%). However, PS I emission is strongly Stokes shifted and thus visible in a resonant excitation experiment. By contrast, resonantly excited PS II emission is *homogeneously broadened* and observable mainly through vibrational sideband structures V1/V2 etc. Vibrational sidelines have only ~10% of the intensity of the resonant emission and thus, PS I emission will be an order of magnitude *more visible* than PS II. Additionally, at temperatures when strong SHB occurs, PS II emission originates from (weaker) phonon wing excitation (see Fig. 6), leading to a further bias to PS I emission over that of PS II. Fig. 10 shows that this enhancement can be over an order of magnitude.

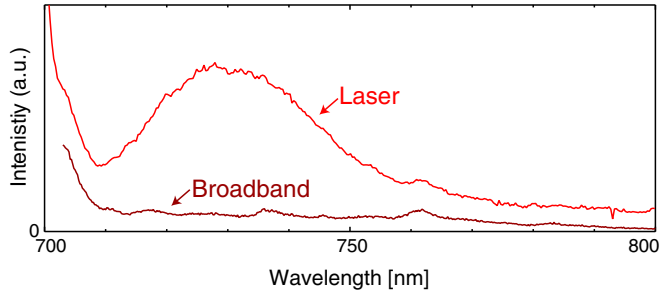


**Fig. 10.** Selective emission at 8 K of the *T. vulcanus* PS II sample utilised in Fig. 9, excited by either a laser at 698 nm (70 mW/cm$^2$) or broadband excitation (6 μW/cm$^2$) at the same wavelength. Spectra are scaled to have comparable CP47 V1/V2 FLN features (see text).

Overall, we can look to engineer well-defined protocols that leads to a ~$10^2$–$10^4$ bias to PS I over PS II in (detectable) emission intensity, whilst maintaining the distinctive difference in spectral characteristics between the two photosystems. The methodology applies equivalently to the various forms of PS I and LHCIs that may be present in a plant PS II preparation. It utilises the absorption and emission characteristics of their 'red trap' states, which are precisely those states whose absorptions interfere with spectroscopic characterisation of the DRS state in PS II core complexes.

The situation in PS I contaminated cyanobacterial PS II is different, as in these organisms the PS II 'red traps' are not located in LHCIs attached to the PS I core as in the plant case but within the PS I core itself. There are usually no LHCs in cyanobacteria. The number, detailed nature and excitation transfer between the 'red traps' in PS I in *T. elongatus* for its monomeric/trimeric etc. forms are still under discussion [13,30]. It has been suggested [42] that the 'red traps' in PS I may be associated with pigment trimers and tetramers as well as dimers. Riley et al. [29] have shown that degraded forms of PS I of *T. elongatus* absorb less strongly in the red region, indicating a disruption of the 'red traps'. If there are forms of PS I present in a cyanobacterial PS II sample that are significantly different to that in the PS I calibration sample, a systematic error in the estimation of the PS I content can occur. Such a situation may be indicated by a different PS I emission peak position and/or width seen from a PS II sample, compared to that obtained from the PS I calibration sample.

A PS I content determination for cyanobacterial PS II sample containing modified or degraded PS I thus provides only an *effective* PS I content. The determination assumes that the PS I in the PS II has the same properties as the PS I species used in the calibration process. If the modified PS I species present exhibit, via resonant excitation through the 700 nm–730 nm region, a comparable amount of 'red trap' emission (per unit absorption) to that seen for the PS I used for calibration, then the process still effectively monitors PS I-related absorption in this spectral region important to the study of the DRS, which is the primary goal of this work.

### 3.2. Quantification of PS1 in PS II samples

The phenomenology developed above leads to the following methodology:

- Excite samples near 700 nm with broadband and/or laser excitation
- Measure emission at LHe and/or $LN_2$ temperatures
- Choose an excitation wavelength inducing comparable PS II & PS I emission intensities
- Calibrate the broad, Stokes shifted PS I emission intensity by adding a known amount of PS I to a PS II sample

- Monitor and calibrate the PS II content via the relatively narrow and distinctive CP47 V1/V2 FLN features

The above approach overcomes a significant difficulty in low temperature fluorescence spectroscopy, where the reproducibility of intensity measurements made on a sample can be poor. The detected intensity is dependent on the precise alignment of the sample relative to the cryostat, the spectrometer and the excitation beam. Additionally there is inherent variability of the optical properties of the frozen glasses to consider. The ability to quantify distinctive features due to both PS I and PS II *in the same spectrum* obviates this limitation.

Our experiments are always performed in a region of very low sample absorbance at the excitation wavelength. The total (CP47 + DRS) molar extinction of plant PS II near 705 nm is ~20,000 $M^{-1}$ $cm^{-1}$ with that of PS I about an order of magnitude higher (see Fig. 2). A highly concentrated PS II core (8 mg/mL chl-a) in a 200 μm cell thickness has an absorbance of <0.1 at 700 nm and thus reabsorption of fluorescence by the sample is minimal.

We have found that useful experiments can be performed at $LN_2$ temperatures. The CP47 V1/V2 FLN features, though broadening significantly (see Supplementary Fig. S2) are still quite distinguishable. At this higher temperature, spectra obtained utilising laser and broadband excitation are virtually identical (Supplementary data Fig. S2). Emission processes are somewhat weaker at 77 K but sensitivity can be regained by using an excitation source of the greater power.

At LHe temperatures, fluorescence quantum efficiencies become higher, particularly for PS II. This leads to an overall increase in sensitivity of the experiment. Additionally SHB process below 30 K, when using laser excitation, leads to weaker PS II V1/V2 features relative to PS I emission (Fig. 10). This allows a smaller fraction of PS I to be identified more reliably via exposing the broad PS I emission, relative to PS II V1/V2 emission.

### 3.2.1. Quantification of PS I in cyanobacterial PS II cores

By using the phenomenology developed above (details of the procedure used are provided in the Supplementary information), Fig. 11 leads to a calibration of the PS I content of the PS II core preparation of the *T. vulcanus* sample utilised in Figs. 9 and 10. The scatter seen around the least-squared fit line in Fig. 12 is due largely to the volumetric errors associated with using very low volumes and viscous samples. The PS I content in the PS II preparation is determined as 1.9%; that is 1.9% of chl-a is present as PS I. As the number of ch-as in a PS I is ~3× that of in PS II for *T. vulcanus*, the fraction of photosystems present as PS I (mole fraction) in the sample is ~0.6%.

We note that this experiment, which was performed at 77 K, does not require a laser and can be performed on a good-quality laboratory spectrofluorimeter. The comparable amplitude of PS I and PS II emission features, when 0.6% of assemblies are PS I (Supplementary Fig. S6), is in accord with the estimates made in Section 3.1 based on molar extinction

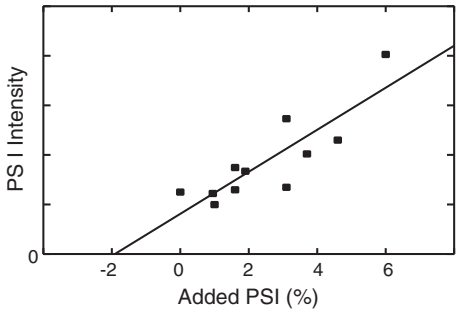


**Fig. 11.** PS I content as measured by PS I emission intensity of a *T. vulcanus* preparation with calibrated amounts of PS I added. Spectra (Fig. S6) were taken at 77 K using 700 nm excitation. The PS I content of the (non-recrystallised) PS II core preparation is determined to be 1.9 ± 0.7% by chl-a as PS I.

of PS I and PS II (Fig. 2) in addition to the relative visibilities of the fluorescence of the two species when resonantly excited near 700 nm.

At 77 K, the practical limit of sensitivity in determining PS I content whilst retaining a PS II FLN calibration feature is ~0.2% of photosystems as PS I. A significant increase in sensitivity towards PS I can however be gained by measuring spectra at 8–10 K and utilising laser excitation to take advantage of SHB processes. The consequent depletion of PS II absorption at the laser wavelength suppresses, very effectively, PS II emission features relative to that of PS I. Fig. 10 demonstrates the dramatic effect of SHB. In the broadband excited spectrum where there is little SHB, there is marginal if any evidence for any PS I content, whereas in the laser excited spectrum, the PS I feature becomes absolutely dominant. Fig. 10 points to a ~10–100 fold increase in sensitivity towards PS I at the lowest temperatures when SHB processes suppress PS II absorption.

Fig. 13 shows the selective emission spectra of *T. vulcanus* PS II cores, sourced from the preparation that had not been recrystallised and those of two preparations prepared by re-dissolving crystallised PS II. Spectra are excited at 698 nm and at 8 K. In the corresponding spectra at 77 K (Supplementary Fig. S7), the PS I emission evident in the regular preparation, which contains mole fraction 0.6% PS I, is far less pronounced. This is due to the SHB process that suppresses PS II FLN emission *not* being active at 77 K. The 698 nm laser spectrum in Fig. 10 of the same PS I contaminated sample shows 2–3× enhancement of the PS I emission feature relative to the PS II FLN features. This was due to the higher power density of the laser excitation utilised and to the laser illumination being made for a longer time before the spectrum was recorded. This allowed SHB processes progress to a stronger depletion of PS II CP47 absorption.

The spectrum of the (a) crystal based sample in Fig. 13 shows a threefold reduction in PS II related emission compared to the non-recrystallised PS II preparation, but the emission may not correspond precisely to that from pure PS I excited at 730 nm. The (b) crystal sample has an order of magnitude less PS I related emission than the non-recrystallised PS II preparation, However, it exhibits a tailing emission in the 700–730 nm region that does not scale with the CP47 V1/V2 FLN features. This indicates an additional fluorescent impurity.

A similar strong tailing of the (b) crystal sample is seen in the 77 K spectra (Supplementary Fig. S7). The 77 K spectra are consistent with the PS I content of both crystal based samples being an order of magnitude or more lower in both the (a) and (b) crystal samples.

The 8 K *T. vulcanus* wavelength dependent emission spectra in Fig. 5 exposes PS I emission in the (b) sample under longer wavelength excitation. However, the parallel changes seen in the 700–730 nm tailing emission, along with the fact that this tail feature is not clearly due to either PS I related species or intact PS II makes further quantification difficult.

### 3.2.2. Quantification of PS I in spinach PS II cores

Experiments were performed on a range of spinach PS II core preparations but in this paper we report the properties of two samples identified as (a) and (b) in detail. It was found that samples prepared from market spinach in winter had far less PS I content than those prepared at other times.

As shown in Figs. 5 and 12, sample (b) has *no measureable PS I content*. Sample (a) has low but measurable content (Fig. 9 and Supplementary Fig. S9). Using a procedure similar to that utilised for *T. vulcanus* samples, the analysis in the Supplementary data establishes that the mole fraction of PS I of the (a) sample is 0.15 ± 0.08% PS I. In contrast to the *T. vulcanus* recrystallised preparation analysis, the PS I content exhibited a very similar emission spectrum to that of our isolated PS I preparation (see Fig. 8) suggesting that the PS I species present was not significantly degraded.

An *upper limit* for the mole fraction of PS I related content of the (b) sample was determined (Supplementary information) to be 0.01%. A comparison of the wavelength dependent emission spectra of the (immeasurably-low) PS I content spinach PS II sample (b) in Fig. 12 with

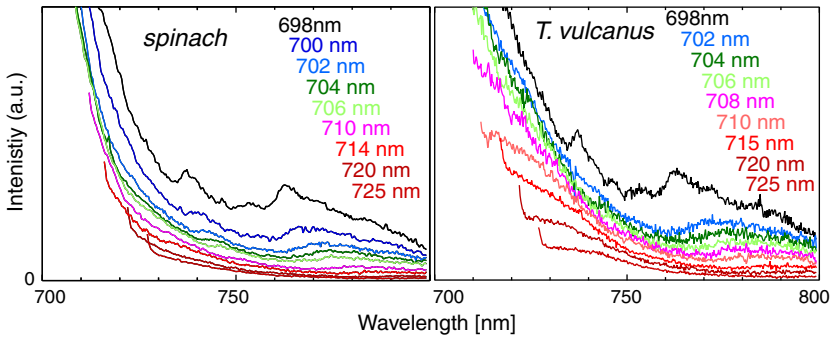


**Fig. 12.** Selective emission spectra at 8 K of ~1 mg/mL chl-a PS II core sample (b) of spinach (left panel) and recrystallised *T. vulcanus* sample (b) (right panel). Laser excitations are at the wavelengths indicated and have an incident power density of 100–400 mW/cm$^2$. Spectra are scaled to the same excitation power density.

the corresponding spectra of sample (a) (Supplementary Fig. S11) where there is a small (0.15%) but easily seen PS I emission component, establishes the 780 nm band in both sets of spectra to have the same intensity, relative to the to the PS II based CP47 V1/V2 FLN features. Consequently, the 780 nm band intensity does not scale with the PS I emission intensity. This helps establish that the 780 nm band is not due to PS I and is due to PS II.

## 4. Discussion

### 4.1. PS II core complex purity

The ability to expose the broad, long wavelength emission near 780 nm in both *T. vulcanus* and spinach has required the identification and quantification of samples containing very low levels of PS I contamination. In the case of *T. vulcanus*, this has only been possible via the availability of recrystallised protein samples. Whereas the DRS in spinach PS II cores has been seen in absorption extending to ~730 nm, parallel measurements have not been possible for *T. vulcanus* or other organisms. Further evidence [43] for similar long-wavelength absorption of closely-related *T. elongatus* PS II comes from light induced $Q_A^-$ formation using >700 nm illumination, but no quantification of the absorption responsible for this photoactivity has been possible due to the interference by absorption from PS I contaminants in the same spectral region.

This paper has gone to considerable lengths to describe and establish protocols by which the PS I related content of a PS II core preparation can be systematically and reliably estimated. Interestingly, useful measurements can be made at $LN_2$ temperatures using a simple broadband spectrofluorimeter. This appears to be a unique analytic application of FLN and SHB phenomenologies.

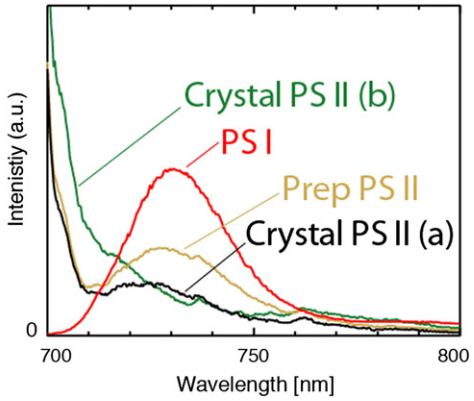


**Fig. 13.** Selective 8 K emission spectra PS II samples (a) and (b) having low PS I content as prepared from recrystallised *T. vulcanus* PS II (green and black traces). The brown trace is the PS II preparation containing 0.6% mole fraction PS I (see text). The three PS II core emission spectra are normalised to the same amplitude of the CP47 V1/V2 FLN features. The red trace is a spectrum of *T. vulcanus* PS I. Spectra are excited at 698 nm with powers of 3–8 mW.

In parallel, the data accumulated have provided strong evidence that it is indeed PS II that is responsible for the ~780 nm emission seen. We have observed similar long wavelength emission spectra in PS II core preparations isolated from other organisms. In each case, the magnitude of the emission, relative to the benchmarking PS II FLN features, is comparable. We have noted that the long-wavelength emission persists to $LN_2$ temperatures before being overwhelmed by the growing tail of the higher energy PS II emissions. This indicates that even at these temperatures, equilibration of the DRS with the CP47 emitting pigments may not occur. This possibility requires more precise spectra and a quantitative analysis of the temperature dependence.

The recrystallised *T. vulcanus* preparation shows entirely analogous emission to that seen in low-PS I spinach PS II cores (Fig. 12). The 780 nm feature is visible in non-recrystallised preparations, but less visible due to the increased presence of PS I emission. However, in each case, the relative intensity of the 780 nm band scales with CP47 V1/V2 FLN features but not with the PS I emission in these samples. We feel that there is little reason to suspect that the long wavelength emission is not a characteristic of all PS II centres in a sample.

### 4.2. Long wavelength emission from PS II

If the dipole strength of the DRS is ~0.15 of that of $Q_y$ in chl-a as reported [14], its radiative lifetime would be ~100 ns. Any emission from the DRS would need to compete with charge separation and other non-radiative processes. The latter are likely to be much faster. With 698 nm excitation, the DRS and PS II CP47 absorption strength (at LHe temperatures) are comparable (Section 3.1.4). In Fig. 12, it is clear that the PS II FLN emission features have, cumulatively, a comparable intensity to the long wavelength emission.

If we estimate resonant emission QE from the CP47 proximal antenna to be ~10% and the total sideband intensity (i.e. the integral of the CP47 V1/V2 FLN features etc.) to be ~10% of the resonant emission as argued in Section 3.1.1, then prima face, the QE of the long wavelength emission would be of the order of 1%. However, in Fig. 12, we have established that PS II FLN features are suppressed by SHB processes. Thus the actual QE of long wavelength emission is likely to be 1–2 orders of magnitude lower than the 1% estimate above. This then would predict a lifetime of the long wavelength emission to be in the range of 10–100 ps.

Vasil'ev et al. [44] suggested some time ago that excitation transfer between the proximal antennae CP43 and CP47 to the reaction centre would be slow, based on inter-pigment distances in early crystallographic data. We interpreted [33] SHB data on PS II core complexes to confirm that these rates were indeed slow at low temperatures. From the data in the current paper, it is evident that emission from the reaction centre in PS II core complexes of both plants and cyanobacteria peaks near

780 nm, whereas emission from the CP43 and CP47 antennae peaks at ~1700 $cm^{-1}$ to higher energy, in the 685 nm to 695 nm region. Thus these emission processes must be strongly decoupled. The well-known *strong* temperature dependence of PS II core emission suggests that there may be thermally activated excitation transfer process from the proximal antennae to the reaction centre. The DRS clearly needs to be included in the modelling of such processes and the detailed nature of the emission processes in PS II thus needs to be re-examined on this basis.

The large Stokes shift between the putative peak of the DRS absorption reported (705 nm) and the long wavelength emission reported here (780 nm) is more than expected with a nominal origin of a strongly homogenously broadened DRS absorption assigned to be near 730 nm. We note that the reported DRS peak position of 705 nm was *not directly observed* but estimated via a Gaussian least-squared fitting analysis, which also modelled CP47 proximal antenna absorption. However, the width of the new emission feature appears comparable to that of the DRS (500 $cm^{-1}$ FWHM).

It may be that the DRS absorption is significantly broader, extending to higher energies and that the true linewidth of the long wavelength emission has not been fully revealed by the limited analysis in Supplementary Fig. S5. More detailed spectra extending beyond 800 nm are required. A broader linewidth of the DRS and the long wavelength emission would bring our understanding more into line with the (higher energy) charge transfer state in PS II core complexes identified [45] by Stark modulation spectroscopy.

## 5. Conclusions

A quantitative determination of the spectral features, function and significance of the DRS and its putative long-wavelength emission system will require more detailed experiments and very likely, the use of PS II preparations containing less than 0.08% mole fraction PS I related contaminants. The calibrations, procedures and protocols developed in this paper can serve to effectively monitor the purity of PS II core samples utilised.

The uncovering of the long wavelength emission at 780 nm in PS II core complexes helps open the possibility of an examination of any functional role of the DRS state in more detail.

## Acknowledgements

We would like to thank Juniali Negi for her efforts during the early phase of this project. E.K. would like to thank Roberta Croce and Petra Fromme for useful discussions. We also recognise the support of the Australian Research Council through grant DP110104565 (E.K.) and MEXT/JSPS of Japan through a Grant-in-Aid for Specially Promoted Research (No. 24000018; J.R.S.).

## Appendix A. Supplementary data

Supplementary data to this article can be found online at http://dx.doi.org/10.1016/j.bbabio.2013.09.008.

## References

[1] O. Nanba, K. Satoh, Isolation of a photosystem II reaction center consisting of D-1 and D-2 polypeptides and cytochrome *b*-559, Proc. Natl. Acad. Sci. 84 (1987) 109–112.
[2] E. Krausz, N. Cox, S.P. Arskold, Spectral characteristics of PS II reaction centres: as isolated preparations and when integral to PS II core complexes, Photosynth. Res. 98 (2008) 207–217.
[3] Y. Umena, K. Kawakami, J.R. Shen, N. Kamiya, Crystal structure of oxygen-evolving photosystem II at a resolution of 1.9 angstrom, Nature 473 (2011) 55–60.
[4] M.R. Razeghifard, M. Chen, J.L. Hughes, J. Freeman, E. Krausz, T. Wydrzynski, Spectroscopic studies of photosystem II in chlorophyll *d*-containing *Acaryochloris marina*, Biochemistry 44 (2005) 11178–11187.
[5] E. Krausz, J.L. Hughes, P. Smith, R. Pace, S. Peterson Årsköld, Oxygen-evolving photosystem II core complexes: a new paradigm based on the spectral identification of the charge-separating state, the primary acceptor and assignment of low-temperature fluorescence, Photochem. Photobiol. Sci. 4 (2005) 744–753.
[6] B. Gobets, R. van Grondelle, Energy transfer and trapping in photosystem I, Biochim. Biophys. Acta 1507 (2001) 80–99.
[7] E. Schlodder, M. Hussels, M. Cetin, N.V. Karapetyan, M. Brecht, Fluorescence of the various red antenna states in photosystem I complexes from cyanobacteria is affected differently by the redox state of P700, Biochim. Biophys. Acta Bioenerg. 1807 (2011) 1423–1431.
[8] E. Krausz, J.L. Hughes, P.J. Smith, R.J. Pace, S. Peterson Årsköld, Assignment of the low-temperature fluorescence in oxygen-evolving photosystem II, Photosynth. Res. 84 (2005) 193–199.
[9] E.G. Andrizhiyevskaya, A. Chojnicka, J.A. Bautista, B.A. Diner, R. van Grondelle, J.P. Dekker, Origin of the F685 and F695 fluorescence in photosystem II, Photosynth. Res. 84 (2005) 173–180.
[10] A. Murakami, Quantitative analysis of 77 K fluorescence emission spectra in *Synechocystis* sp. PCC 6714 and *Chlamydomonas reinhardtii* with variable PS I/PS II stoichiometries, Photosynth. Res. 53 (1997) 141–148.
[11] X.C. Qin, W.D. Wang, K.B. Wang, Y.Y. Xin, T.Y. Kuang, Isolation and characteristics of the PSI-LHCI-LHCII supercomplex under high light, Photochem. Photobiol. 87 (2011) 143–150.
[12] T. Morosinotto, R. Bassi, Antenna system of higher plants' photosystem I and its interaction with the core complex, in: G. Renger (Ed.), Primary Processes of Photosynthesis, Part 1: Principles and Apparatus, The Royal Society of Chemistry, 2008.
[13] R. Fromme, I. Grotjohann, P. Fromme, Structure and function of photosystem I, in: G. Renger (Ed.), Primary Processes of Photosynthesis, Part 2, 2008.
[14] J.L. Hughes, P. Smith, R. Pace, E. Krausz, Charge separation in photosystem II core complexes induced by 690–730 nm excitation at 1.7 K, Biochim. Biophys. Acta 1757 (2006) 841–851.
[15] J.L. Hughes, P.J. Smith, R.J. Pace, E. Krausz, Low energy absorption and luminescence of higher plant photosystem II core samples, J. Lumin. 122–123 (2007) 284–287.
[16] J.L. Hughes, E. Krausz, Electronic spectroscopy, in: R.A. Scott, C.M. Lukehart (Eds.), Application of Physical Methods to Inorganic and Bioinorganic Chemistry, John Wiley & Sons, Ltd., 2007.
[17] E. Krausz, Selective and differential optical spectroscopies in photosynthesis, Photosynth. Res. (2013). (http://dx.doi.org/10.1007/s11120-013-9881-7).
[18] E. Krausz, C. Tomkins, H. Adler, An efficient helium flow tube for low-temperature experiments, J. Phys. E Sci. Instrum. 15 (1982) 1167–1168.
[19] P.J. Smith, S. Peterson, V.M. Masters, T. Wydrzynski, S. Styring, E. Krausz, R.J. Pace, Magneto-optical measurements of the pigments in fully active photosystem II core complexes from plants, Biochemistry 41 (2002) 1981–1989.
[20] J.E. Mullet, J.J. Burke, C.J. Arntzen, Chlorophyll proteins of photosystem I, Plant Physiol. 65 (1980) 814–822.
[21] R. Bassi, D. Simpson, Chlorophyll–protein complexes of barley photosystem I, Eur. J. Biochem. 163 (1987) 221–230.
[22] J.R. Shen, Y. Inoue, Binding and functional properties of 2 new extrinsic components, cytochrome-C-550 and a 12-kDa protein, in cyanobacterial photosystem II, Biochemistry 32 (1993) 1825–1832.
[23] J.R. Shen, N. Kamiya, Crystallization and the crystal properties of the oxygen-evolving photosystem II from *Synechococcus vulcanus*, Biochemistry 39 (2000) 14739–14744.
[24] J.L. Hughes, E. Krausz, Novel characteristics of persistent spectral hole-burning and hole-filling in photosystem II core complexes, J. Lumin. 127 (2007) 239–244.
[25] J.L. Hughes, R. Picorel, M. Seibert, E. Krausz, The assignment and photophysical behavior of the low-energy chlorophyll states in the CP43 proximal antenna protein of higher plant photosystem II, Biochemistry 45 (2006) 12345–12357.
[26] V. Zazubovich, S. Matsuzaki, T.W. Johnson, J.M. Hayes, P.R. Chitnis, G.J. Small, Red antenna states of photosystem I from cyanobacterium *Synechococcus elongatus*: a spectral hole burning study, Chem. Phys. 275 (2002) 47–59.
[27] R. Purchase, S. Volker, Spectral hole burning: examples from photosynthesis, Photosynth. Res. 101 (2009) 245–266.
[28] R. Jankowiak, M. Reppert, V. Zazubovich, J. Pieper, T. Reinot, Site selective and single complex laser-based spectroscopies: a window on excited state electronic structure, excitation energy transfer, and electron–phonon coupling of selected photosynthetic complexes, Chem. Rev. 111 (2011) 4546–4598.
[29] K.J. Riley, T. Reinot, R. Jankowiak, P. Fromme, V. Zazubovich, Red antenna states of photosystem I from cyanobacteria *Synechocystis* PCC 6803 and *Thermosynechococcus elongatus*: single-complex spectroscopy and spectral hole-burning study, J. Phys. Chem. B 111 (2007) 286–292.
[30] M. Yang, A. Damjanovic, H.M. Vaswani, G.R. Fleming, Energy transfer in photosystem I of cyanobacteria *Synechococcus elongatus*: model study with structure-based semi-empirical Hamiltonian and experimental spectral density, Biophys. J. 85 (2003) 140–158.
[31] J.L. Hughes, B. Conlon, T. Wydrzynski, E. Krausz, The assignment of Qy(1,0) vibrational structure and Q(x) for chlorophyll a, Phys. Procedia 3 (2010) 1591–1599(1100).
[32] M. Ratsep, A. Freiberg, Electron–phonon and vibronic couplings in the FMO bacteriochlorophyll a antenna complex studied by difference fluorescence line narrowing, J. Lumin. 127 (2007) 251–259.
[33] J.L. Hughes, B.J. Prince, E. Krausz, P.J. Smith, R.J. Pace, H. Riesen, Highly efficient spectral hole-burning in oxygen-evolving photosystem II preparations, J. Phys. Chem. B 108 (2004) 10428–10439.
[34] E. Krausz, J.L. Hughes, P.J. Smith, R.J. Pace, S. Peterson Årsköld, The reaction center of PSII in oxygen-evolving preparations, 13th International Conference on Photosynthesis, Montreal, Canada, 2004.
[35] F.L. de Weerd, M.A. Palacios, E.G. Andrizhiyevskaya, J.P. Dekker, R. van Grondelle, Identifying the lowest electronic states of the chlorophylls in the CP47 core antenna protein of photosystem II, Biochemistry 41 (2002) 15224–15233.

[36] R.I. Personov, The historical development of high-resolution selective spectroscopy of organic molecules in solids, in: C. Gooijer, F. Ariese, J.W. Hofstraat (Eds.), Shpol'skii Spectroscopy and Other Site-Selection Methods, Wiley-Interscience, New York, 2000, pp. 1–18.
[37] J.L. Hughes, E. Krausz, P.J. Smith, R.J. Pace, H. Riesen, Probing the lowest energy chlorophyll *a* states of photosystem II via selective spectroscopy: new insights on P680, Photosynth. Res. 84 (2005) 93–98.
[38] H. Koloczek, J. Fidy, J.M. Vanderkooi, Fluorescence line-narrowing spectra of Zn-cytochrome c. Temperature dependence, J. Chem. Phys. 87 (1987) 4388–4394.
[39] V.M. Agranovich, R.M. Hochstrasser, Spectroscopy and excitation dynamics of condensed molecular systems, North-Holland Pub. Co.; Sole distributors for the USA and Canada, Elsevier Science Pub. Co., Amsterdam; New York; New York, N.Y., 1983
[40] W.E. Moerner, Persistent spectral hole-burning: science and applications, Topics in Current Physics, Springer-Verlag, Berlin, Heidelberg, 1988, p. 315.
[41] M.L. Groot, E.J.G. Peterman, P.J.M. Vankan, I.H.M. Vanstokkum, J.P. Dekker, R. Van Grondelle, Temperature-dependent triplet and fluorescence quantum yields of the photosystem II reaction center described in a thermodynamic model, Biophys. J. 67 (1994) 318–330.
[42] S. Vaitekonis, G. Trinkunas, L. Valkunas, Red chlorophylls in the exciton model of photosystem I, Photosynth. Res. 86 (2005) 185–201.
[43] J.L. Hughes, N. Cox, A.W. Rutherford, E. Krausz, T.L. Lai, A. Boussac, M. Sugiura, D1 protein variants in photosystem II from *Thermosynechococcus elongatus* studied by low temperature optical spectroscopy, Biochim. Biophys. Acta Bioenerg. 1797 (2010) 11–19.
[44] S. Vasil'ev, P. Orth, A. Zouni, T.G. Owens, D. Bruce, Excited-state dynamics in photosystem II: insights from the X-ray crystal structure, Proc. Natl. Acad. Sci. 98 (2001) 8602–8607.
[45] E. Romero, B.A. Diner, P.J. Nixon, W.J. Coleman, J.P. Dekker, R. van Grondelle, Mixed exciton–charge-transfer states in photosystem II: stark spectroscopy on site-directed mutants, Biophys. J. 103 (2012) 185–194.
[46] F. Muh, A. Zouni, Extinction coefficients and critical solubilisation concentrations of photosystems I and II from *Thermosynechococcus elongatus*, Biochim. Biophys. Acta Bioenerg. 1708 (2005) 219–228.